

# SUPPLEMENTARY MATERIAL

## Supplementary methods

### Tumour analyses

TMA sections (4 µm) were stained with a multimarker panel including primary antibodies against CD3, CD8 and CD68 using fluorescence-based multiplex immunohistochemistry following the protocol described in (1). Briefly, a 5-plex stain was designed using the Opal™ Multiplex IHC method (PerkinElmer/Akoya, USA). Deparaffinization was performed in xylene, followed by hydration in graded alcohols. The Dako PT link module was used for heat-induced epitope retrieval for 20 min at 97 °C using the EnVision™ FLEX Target Retrieval Solution (3-in-1) pH 9 (Agilent/Dako, USA, catalogue number K800421-2) in 65 °C preheat mode. The Dako PT link module was also used for antibody stripping for 20 min at 97 °C using AR9 buffer (PerkinElmer/Akoya, USA, catalogue number AR9001KT) in 80 °C preheat mode (AR6 (PerkinElmer/Akoya, USA, catalogue number AR6001KT) was used prior to staining of cytokeratins/E-cadherin). Antibody staining was done using the Opal™ 4 Color Manual IHC Kit and an Opal 620 reagent pack (PerkinElmer/Akoya, USA, catalogue numbers NEL810001KT and FP1495001KT; kit contains blocking solution/antibody diluent, secondary antibody, Opal fluorophores and DAPI) according to the manufacturer's recommendations. Briefly, in each cycle following antigen retrieval/antibody stripping, tissue sections were incubated for 10 minutes with blocking solution prior to incubation with primary antibody solution for 30 minutes. After 3x2 minutes washes in TBST, the secondary antibody (PerkinElmer/Akoya, USA) was incubated for 10 minutes. A new 3x2 minutes wash cycle was performed before incubation with Opal fluorophore for 10 minutes. A final 3x2 minutes wash cycle was performed prior to antibody stripping. Monoclonal primary antibodies were chosen to facilitate reproducibility of the study since they are generally more specific than polyclonal antibodies, easier to reproduce and less affected by formalin fixation bias. The specific clones were selected based on comparative testing and quality assessments by the Nordic immunohistochemical Quality Control (NordiQC; nordiqc.org) organisation. The following primary antibodies and Opal fluorophores were used (in the order they were stained): CD68 (1:6000, clone KP1, Agilent/Dako, catalogue number M081401-2; detected by Opal 620 at 1:125); CD3 (1:400, clone F7.2.38, Agilent/Dako, catalogue number M725401-2; detected by Opal 570 at 1:100), CD8 (1:600, clone C8/144B, Agilent/Dako, catalogue number M710301-2; detected by Opal 520 at 1:100). The tissue was hybridised with a cocktail of epithelial markers in the last staining cycle to facilitate accurate epithelial

36 segmentation by the digital image analysis algorithm (anti-pan Cytokeratin (1:2000, clone C-  
37 11, Abcam, UK, catalogue number ab7753), anti-pan Cytokeratin Type I/II (1:1000, clone  
38 AE1/AE3, Thermo Fisher Scientific, USA, catalogue number MA5-13156) and anti-E-  
39 cadherin (1:10000, clone 36, BD Biosciences, USA, catalogue number 610182)); detected by  
40 Opal 690 at 1:100. DAPI (PerkinElmer/Akoya, USA) was used as counterstain prior to slide  
41 mounting with ProLong Diamond Antifade Mountant (Invitrogen/Thermo Fisher Scientific,  
42 USA, catalogue number P36970). All fluorophores were included in singleplex stains to  
43 create spectral libraries to unmix individual spectral signatures in the multiplex. The spectral  
44 signature of the tissue autofluorescence was obtained from a slide not probed with any  
45 fluorophore but otherwise treated as the other library stains. All markers were optimised prior  
46 to multiplex staining as follows. A separate test TMA (n = tissue cores = 166; 83 unique  
47 samples in duplicate), consisting of cores taken from a variety of tissues, including colorectal  
48 (normal (n = 12; 6 in duplicate) and cancer (n = 82; 41 in duplicate)) and lymph node tissues  
49 (n = 6; 3 in duplicate), as well as a broad variety of other normal tissues and cancers  
50 (including normal testis, prostate, liver, appendix, spleen, thymus and tonsil) was stained by  
51 conventional brown staining (3,3'-diaminobenzidine) for each marker individually to  
52 determine optimal antibody concentrations. Antibodies were then paired with an Opal  
53 fluorophore, and the test TMA was fluorescently labelled by each marker individually, along  
54 with DAPI (monoplex stain). A negative control experiment was performed where the primary  
55 antibody was omitted from one slide. These stains were compared to the brown stains to  
56 determine if antibody, or Opal fluorophore concentrations, needed fine-tuning to achieve  
57 optimal specificity and linear dynamic range. When optimal concentrations for fluorescent  
58 labelling were determined, a multiplex stain was performed on the test TMA and compared to  
59 the monoplex stains to ensure proper staining also when performing the sequential multiplex  
60 staining procedure (e.g., control for potential antigen blocking by the TSA reagent). Multiplex  
61 stains were optimised to achieve signal balance between the fluorophores to avoid potential  
62 signal bleedthrough and facilitate accurate unmixing of the fluorophore spectras. Finally,  
63 strip-testing was performed on the test TMA to ensure that antibodies were properly stripped  
64 away between each staining cycle. This was done by a regular cycle of staining with each  
65 antibody individually, followed by heat treatment in the PT link module and another cycle of  
66 staining using blocking solution, secondary antibody and the next fluorophore in the  
67 multiplex, but this time omitting any primary antibody. Images were then taken to verify that  
68 no signal above background values was detected from the second fluorophore applied.

### 69 **Image acquisition and digital image analysis**

70 Multispectral images of the TMAs were acquired at 20x magnification (0.5  $\mu\text{m}/\text{pixel}$ ) using the  
71 Vectra 3.0 Automated Quantitative Pathology Imaging System, 200 slides (Vectra software

72 version 3, PerkinElmer/Akoya, USA). Four images (2x2) were taken of each tissue core. The  
73 standard setup for multispectral imaging was used, i.e. images were taken at 35 wavelengths  
74 across the five excitation filters. Exposure times for the various filters were as follows; DAPI:  
75 50ms, FITC: 150ms, Cy3: 150ms, Texas Red: 150ms, Cy5: 150ms (however, of note, the  
76 system automatically limits the exposure if a fluorophore is in danger of becoming  
77 overexposed and this is later automatically adjusted for during calculations of fluorophore  
78 intensities in the accompanying inForm software). Multispectral image analysis of the  
79 multiplex stains was carried out with the inForm Image Analysis Software (version 2.3, Akoya  
80 Biosciences). Representative training images were initially loaded and spectrally unmixed  
81 with the spectral libraries generated from the individual fluorophore library stains and the  
82 autofluorescence slide. A machine-learning algorithm was then trained by user-specified  
83 tissue annotations aided by the epithelial markers' signal to segment tumour tissue *versus*  
84 stromal tissue and background. The segmentation of individual cells was based on the  
85 nuclear DAPI signal (specifically, in inForm, the minimum size for nuclei was set to 80 pixels,  
86 typical size was set to 320 pixels, minimum signal was set to 0.18, splitting was set to 2.26,  
87 growth of nuclei set to 0.35 and membrane signal was used to aid segmentation). CD68  
88 signal was included for segmentation of cytoplasm in cells where this marker was detected  
89 (specifically, inner distance to the nucleus was set to 0 pixels, outer distance to the nucleus  
90 was set to 6 pixels, minimum size was set to 20 pixels, minimum signal was set to 0.3 with  
91 no bounds on the maximum). Membrane segmentation was aided by the signals from CD8  
92 (full-scale count set to 10.9), CD3 (full-scale count set to 9.0) and the epithelial markers (full-  
93 scale count set to 8.7) with a maximum distance to membrane set to 12 pixels. See  
94 supplementary Figure S1 for representative examples from the image analysis in inForm. A  
95 review of all images was performed after batch processing. The raw file containing mean  
96 intensity signals per cell in the entire cohort was analysed using R software, version 3.3.1 (R  
97 Foundation for Statistical Computing, Vienna, Austria). No R packages (besides base  
98 packages) were used. A custom script was written to score cells as positive for a marker if  
99 mean signal intensities were above the threshold set for the marker. Cell densities were then  
100 calculated based on the number of positive cells within the tissue category (tumour epithelial  
101 tissue or stroma) or within the tissue core as a whole. For scoring cell positivity, the mean  
102 fluorescence intensity within the nuclear area of cells was used for CD3 and CD8, while  
103 mean cellular scores (within the nuclear, cytoplasmic and membrane area combined) were  
104 used for CD68. CD3 and CD8 cells were generally small and often tightly packed; thus, using  
105 the tighter segmentation of the nuclear area resulted in optimal scoring of these cells.  
106 However, using the entire cell area for mean fluorescence intensity-based scoring was  
107 visually found to be better for the generally larger CD68 macrophages (this is why only CD68  
108 was used during cytoplasm segmentation). Positivity thresholds were set based on manual

109 inspection of representative images and after evaluating the expression distribution across all  
110 cells. To check the thresholds set, we also tested scoring cells with one threshold set below  
111 and one above the thresholds used to procure the final data. The data produced by using the  
112 lower and higher thresholds correlated well for each marker (Spearman's rho 0.84 - 0.93).

### 113 Molecular alterations

114 For correct interpretation of *BRAF* V600E status, we assembled results from previous  
115 immunohistochemistry (IHC) for *BRAF* V600E (2), *BRAF* V600 pyrosequencing (3) and  
116 targeted *BRAF* sequencing in a customized Ampliseq hotspot gene panel (4). For  
117 inconsistent cases, pyrosequencing was redone before a final consensus was made. Eight  
118 cases were mutated according to IHC, but wildtype according to DNA based methods, these  
119 were considered wildtype. Four cases were mutated according to IHC and pyrosequencing,  
120 but wildtype according to hotspot panel sequencing with low variant allele frequency in three  
121 cases; these were considered mutated.

122 Results from previous pyrosequencing of *KRAS* codon 12 and 13 (3) and hotspot gene panel  
123 sequencing were compared (4). Pyrosequencing was redone for inconsistent results. Three  
124 cases were *KRAS* mutated according to pyrosequencing, but wildtype according to hotspot  
125 panel sequencing with low variant allele frequency; these were considered mutated. Two  
126 cases were removed from the final *KRAS* interpretation status due to inconsistent results.

127

- 128 1. Lopes N, Bergsland CH, Bjørnslett M, Pellinen T, Svindland A, Nesbakken A, et al. Digital  
129 image analysis of multiplex fluorescence IHC in colorectal cancer recognizes the prognostic value of  
130 CDX2 and its negative correlation with SOX2. *Lab Invest.* 2020;100(1):120-34.
- 131 2. Aasebo KO, Dragomir A, Sundstrom M, Mezheyeuski A, Edqvist PH, Eide GE, et al.  
132 Consequences of a high incidence of microsatellite instability and BRAF-mutated tumors: A  
133 population-based cohort of metastatic colorectal cancer patients. *Cancer Med.* 2019;8(7):3623-35.
- 134 3. Sorbye H, Dragomir A, Sundstrom M, Pfeiffer P, Thunberg U, Bergfors M, et al. High BRAF  
135 Mutation Frequency and Marked Survival Differences in Subgroups According to KRAS/BRAF  
136 Mutation Status and Tumor Tissue Availability in a Prospective Population-Based Metastatic  
137 Colorectal Cancer Cohort. *PLoS One.* 2015;10(6):e0131046.
- 138 4. Nunes L, Aasebo K, Mathot L, Ljungstrom V, Edqvist PH, Sundstrom M, et al. Molecular  
139 characterization of a large unselected cohort of metastatic colorectal cancers in relation to primary  
140 tumor location, rare metastatic sites and prognosis. *Acta Oncol.* 2020;59(4):417-26.

141

142

## Supplementary tables

**TABLE S1** Unadjusted non-parametric analysis of correlations between CD3, CD8 and CD68 tumour immune cell densities and clinic-pathological variables in a Scandinavian population-based cohort of metastatic colorectal cancer patients

Characteristics	Missing n	Medians	CD3		CD8		CD68	
			p-value	Medians	p-value	Medians	p-value	
Age (years) < 75/> 75		56.1/ 70.3	0.163	36.9/ 45.9	0.090	46.6/ 35.0	0.165	
Gender Female/Male		60.2/ 58.9	0.820	41.2/ 38.9	0.577	40.0/ 43.3	0.587	
PS ECOG 0-1/>1		56.3/ 63.4	0.362	41.6/ 35.1	0.974	45.3/ 39.4	0.488	
Primary tumour location Left / Right	7	53.9/ 65.5	0.200	32.2/ 50.5	<b>0.001</b>	40.4/ 42.7	0.698	
Metastatic site								
Liver absent/present		55.7/ 62.3	0.879	53.5/ 33.0	<b>0.002</b>	39.4/ 41.6	0.834	
Lung absent/present		59.2/ 63.4	0.719	42.4/ 34.8	0.309	42.7/ 37.7	0.634	
Lymph node absent/present		62.9/ 53.3	0.387	37.5/ 47.4	0.159	39.1/ 47.1	0.431	
Peritoneum absent/present		63.4/ 45.6	0.219	40.6/ 39.4	0.882	43.4/ 29.1	0.392	
Bone absent/present		59.5/ 63.4	0.575	40.8/ 34.7	0.667	43.4/ 17.4	<b>0.010</b>	
Synchronous metastases no/yes		63.3/ 56.3	0.920	43.0/ 35.1	0.632	35.8/ 45.3	0.396	
Primary tumour resected no/yes		78.0/ 58.7	0.271	36.9/ 40.8	0.919	40.1/ 41.3	0.679	
Secondary metastasis surgery no/yes	1	58.3/ 69.0	0.200	38.5/ 51.4	0.227	39.6/ 50.8	0.311	
Preoperative radiotherapy no/yes		59.5/ 65.4	0.734	40.8/ 30.6	0.834	40.5/ 43.4	0.573	
Tumour grade 1-2/3	15	64.3/ 53.7	0.241	38.5/ 47.2	0.669	39.2/ 52.8	0.242	
KRAS wildtype/mutation	15	65.7/ 50.1	0.066	43.0/ 37.2	0.520	41.1/ 46.4	0.738	
BRAFV600E wildtype/mutation		56.3/ 62.7	0.391	37.0/ 47.2	0.065	40.5/ 42.6	0.311	
MSS/MSI	1	54.8/102.4	<b>0.041</b>	35.1/141.4	<b>&lt; 0.001</b>	40.4/ 55.7	0.089	
CDX2 positive/negative	2	59.5/ 62.7	0.846	38.7/ 44.1	0.227	40.4/ 51.3	0.366	
APC wildtype/mutation	50	61.0/ 72.7	0.774	43.9/ 31.4	<b>0.033</b>	49.4/ 41.9	0.828	
TP53 wildtype/mutation	50	67.5/ 55.9	0.794	38.7/ 40.8	0.814	46.6/ 42.6	0.414	
PIK3CA wildtype/mutation	50	60.6/ 69.6	0.736	36.0/ 60.1	<b>0.027</b>	42.7/ 54.3	0.448	
SMAD4 wildtype/mutation	50	65.3/ 55.2	0.353	39.4/ 42.6	0.317	46.6/ 33.0	0.181	
			<b>rho</b>	<b>p-value</b>	<b>rho</b>	<b>p-value</b>	<b>rho</b>	<b>p-value</b>
CD68 density		0.25	<b>&lt; 0.001</b>	0.26	<b>&lt; 0.001</b>			
Age (years)		0.10	<b>0.038</b>	0.10	<b>0.030</b>	-0.05	0.344	

*Abbreviations:* Median: median density of tumour infiltrating immune cells per mm<sup>2</sup>; p-value: determined by non-parametric Mann-Whitney U test, except for continuous variables determined by Spearman's rank correlation; rho; Spearman's rank correlation coefficient; PS ECOG: performance status score developed by Eastern Cooperative Oncology Group; Right-sided: Site of primary colon cancer in ascending colon and transversum; Left-sided: Site of primary colon cancer in descending colon, sigmoid and rectum; Synchronous metastases: within six months after initial diagnoses

**TABLE S2** Results from adjusted linear regressions of tumour infiltrating CD3 and CD8 lymphocytes and CD68 macrophages with respect to clinical and pathological variables in a Scandinavian population-based cohort of 376 metastatic colorectal cancer patients

Variables	CD3 tumour density			CD8 tumour density			CD68 tumour density		
	B	95 % CI	p-value	B	95 % CI	p-value	B	95 % CI	p-value
Age > 75 years	0.55	(-0.84, 1.95)	0.435	0.56	(-0.69, 1.80)	0.382	-0.93	(-2.46, 0.61)	0.235
Female	-0.06	(-1.33, 1.22)	0.930	-0.80	(-1.94, 0.34)	0.167	-0.38	(-1.79, 1.02)	0.590
PS ECOG > 1	0.57	(-0.86, 2.00)	0.435	0.23	(-1.05, 1.51)	0.722	0.94	(-0.63, 2.51)	0.239
Right-sided	1.44	(-0.02, 2.91)	0.053	0.95	(-0.37, 2.25)	0.159	0.03	(-1.58, 1.64)	0.972
Liver metastases	-0.26	(-1.71, 1.19)	0.725	-1.31	(-2.60, -0.01)	<b>0.048</b>	-0.34	(-1.94, 1.25)	0.673
Lung metastases	-0.63	(-2.16, 0.92)	0.425	-0.08	(-1.46, 1.29)	0.904	0.13	(-1.56, 1.82)	0.881
Lymph node metastases	-0.50	(-1.99, 0.98)	0.505	0.18	(-1.15, 1.51)	0.791	0.58	(-1.05, 2.21)	0.486
Peritoneal metastases	-0.60	(-2.31, 1.10)	0.487	-0.53	(-2.06, 1.00)	0.495	-0.48	(-2.35, 1.40)	0.618
Bone metastases	-1.43	(-4.04, 1.19)	0.283	-0.53	(-2.87, 1.80)	0.653	-3.34	(-6.22, -0.47)	<b>0.023</b>
Synchronous metastases	-0.04	(-1.42, 1.35)	0.961	-0.19	(-1.42, 1.05)	0.764	-0.59	(-2.10, 0.93)	0.449
Primary tumour resected	1.58	(-1.05, 4.22)	0.238	0.86	(-1.50, 3.21)	0.475	-1.47	(-4.37, 1.43)	0.319
Secondary metastasis surgery	1.54	(-0.93, 4.01)	0.221	0.94	(-1.27, 3.15)	0.403	1.37	(-1.35, 4.08)	0.324
Preoperative radiotherapy	0.46	(-2.44, 3.35)	0.757	1.54	(-1.05, 4.12)	0.244	-0.92	(-4.10, 2.26)	0.570
Tumour grade 3	-1.02	(-2.75, 0.71)	0.246	-0.88	(-2.43, 0.66)	0.261	0.47	(-1.43, 2.37)	0.624
KRAS mutation	-1.04	(-2.52, 0.44)	0.167	-0.20	(-1.52, 1.12)	0.769	1.39	(-0.24, 3.01)	0.094
BRAFV600E mutation	-0.69	(-2.83, 1.45)	0.526	-0.20	(-2.12, 1.71)	0.835	1.44	(-0.92, 3.79)	0.231
MSI	2.35	(-0.47, 5.16)	0.102	5.44	(2.93, 7.96)	<b>&lt; 0.001</b>	2.45	(-0.65, 5.54)	0.121
CDX2 negative	0.31	(-1.55, 2.17)	0.743	0.25	(-1.41, 1.91)	0.768	-0.39	(-2.43, 1.66)	0.712
APC mutation	0.21	(-1.16, 1.57)	0.768	-0.72	(-1.94, 0.50)	0.244	0.00	(-1.50, 1.50)	0.996
TP53 mutation	0.80	(-0.48, 2.09)	0.218	-0.05	(-1.19, 1.10)	0.938	-0.75	(-2.16, 0.67)	0.299
PIK3CA mutation	0.29	(-1.34, 1.92)	0.728	1.43	(-0.03, 2.89)	0.054	0.22	(-1.57, 2.02)	0.806
SMAD4 mutation	-1.27	(-3.26, 0.72)	0.210	-0.84	(-2.61, 0.94)	0.355	-1.12	(-3.31, 1.06)	0.313

*Abbreviations:* B: Regression coefficient calculated using square root of total number of positive cells per mm<sup>2</sup>; Right-sided: Site of primary colon cancer in ascending colon and transversum; Left-sided: Site of primary colon cancer in descending colon, sigmoid and rectum; MSI: microsatellite instable high; CDX2 negative: loss of CDX2 expression

**TABLE S3** Associations between different treatment decisions and tumour infiltration of CD3 and CD8 lymphocytes and CD68 macrophages in a population-based cohort of metastatic colorectal cancer patients (n = 448)

Chemotherapy	n	CD3		CD8		CD68	
		Median	p-value	Median	p-value	Median	p-value
Prior adjuvant							
Yes	67	40.5	0.046	38.0	0.945	33.2	0.235
No	381	62.1		40.6		41.9	
1 <sup>st</sup> line							
Yes	280	56.3	0.254	38.5	0.313	45.2	0.699
No	168	67.5		45.1		37.5	
1 <sup>st</sup> line combination							
Yes	216	59.6	0.659	37.9	0.596	48.5	0.299
No	64	50.0		43.4		36.9	
2 <sup>nd</sup> line							
Yes	162	61.3	0.523	36.5	0.385	61.8	0.021
No	117	51.1		44.1		32.7	
3 <sup>rd</sup> line							
Yes	73	60.6	0.526	33.1	0.612	74.4	0.267
No	89	63.3		40.6		49.4	

*Abbreviations:* p-value: determined by the non-parametric Mann-Whitney U-test

**TABLE S4** Results from unadjusted Cox regression analyses of overall survival in a population-based Scandinavian cohort of metastatic colorectal cancer patients not given palliative chemotherapy (n = 168)

<b>Variable</b>	<b>n (%)</b>	<b>HR</b>	<b>95 % CI</b>	<b>p-value</b>
<i>BRAFV600E</i> mutation	48 (22)	1.67	(1.20, 2.31)	0.002
CDX2 negative	41 (24)	1.84	(1.28, 2.64)	0.001
MSI	19 (9)	1.76	(1.08, 2.86)	0.024
CD3 density		0.99	(0.97, 1.02)	0.657
CD68 density		1.00	(0.98, 1.03)	0.725
CD8 density		0.98	(0.96, 1.01)	0.173

*Abbreviations:* n: number of patients; HR: hazard ratio; CI: confidence interval; p-value: from likelihood ratio test; MSI-H: microsatellite instable high; CD3 density: square root transformed number of tumour infiltrating CD3 lymphocytes per mm<sup>2</sup> tumour tissue microarray; CD8 density: square root transformed number of tumour infiltrating CD8 lymphocytes per mm<sup>2</sup> tumour tissue microarray; CD68 density: square root transformed number of tumour infiltrating CD68 macrophages per mm<sup>2</sup> tumour tissue microarray

**TABLE S5** Results from Cox regression of progression-free survival in a population-based Scandinavian cohort of 244 metastatic colorectal cancer patients after 1<sup>st</sup> line chemotherapy

Variable	Unadjusted				Fully adjusted (n = 244, e = 234)		
	n/e	HR	95 % CI	p-value	HR	95 % CI	p-value
Age, years	279/269	1.01	(0.99, 1.02)	0.395	1.00	(0.98, 1.01)	0.580
Female	279/269	1.11	(0.87, 1.41)	0.409	0.87	(0.65, 1.15)	0.315
PS ECOG	279/269	2.18	(1.58, 3.00)	< 0.001	1.95	(1.35, 2.83)	< 0.001
Right-sided	276/266	1.02	(0.79, 1.31)	0.878	0.75	(0.55, 1.03)	0.074
Tumour grade 3	273/263	1.85	(1.38, 2.47)	< 0.001	1.74	(1.20, 2.51)	0.004
> 1 metastatic site	279/269	1.41	(1.11, 1.80)	0.005	1.24	(0.93, 1.66)	0.141
Synchronous metastasis	279/269	0.95	(0.75, 1.21)	0.700	0.82	(0.62, 1.09)	0.175
Secondary metastasis surgery	278/268	0.33	(0.22, 0.49)	< 0.001	0.37	(0.23, 0.60)	< 0.001
ALP > UNL	264/254	1.54	(1.20, 1.98)	0.001	1.40	(1.05, 1.88)	0.023
<i>BRAFV600E</i> mutation	279/269	1.40	(1.03, 1.91)	0.032	1.20	(0.79, 1.82)	0.402
<i>KRAS</i> mutation	270/260	0.94	(0.74, 1.21)	0.630	1.55	(1.13, 2.12)	0.007
CDX2 negative	277/267	1.97	(1.41, 2.75)	< 0.001	1.45	(0.94, 2.25)	0.093
MSI-H	278/268	2.11	(1.27, 3.53)	0.004	2.39	(1.15, 4.98)	0.020
CD3 density	279/269	0.99	(0.97, 1.01)	0.303	1.00	(0.98, 1.03)	0.533
CD68 density	279/269	0.98	(0.97, 1.00)	0.111	0.99	(0.97, 1.02)	0.533
CD8 density	279/269	1.00	(0.98, 1.02)	0.948	n.i.		

*Abbreviations:* n: number of patients; e: number of events; HR: hazard ratio; CI: confidence interval; p-value: from likelihood ratio test; PS ECOG: performance status score developed by Eastern Cooperative Oncology Group; Right-sided tumour: Site of colon cancer in ascending colon and transversum; Synchronous metastases: within six months after initial diagnoses; ALP > UNL: Alkaline Phosphatase above upper normal limit; MSI-H: microsatellite instable high; CD3 density: square root transformed number of tumour infiltrating CD3 lymphocytes per mm<sup>2</sup> tumour tissue microarray; CD8 density: square root transformed number of tumour infiltrating CD8 lymphocytes per mm<sup>2</sup> tumour tissue microarray; CD68 density: square root transformed number of tumour infiltrating CD68 macrophages per mm<sup>2</sup> tumour tissue microarray; n.i.: not included

**TABLE S6** Results from fully adjusted Cox regression of overall survival in a population-based Scandinavian cohort of 245 metastatic colorectal cancer patients treated with 1<sup>st</sup> line chemotherapy

<b>n = 245, e = 230</b>			
<b>Variable</b>	<b>HR</b>	<b>95 % CI</b>	<b>p-value</b>
Age, years	1.00	(0.99, 1.01)	0.965
Female	0.66	(0.50, 0.88)	0.005
PS ECOG	2.20	(1.53, 3.15)	< 0.001
Right-sided	0.98	(0.72, 1.33)	0.872
Tumour grade 3	1.72	(1.19, 2.49)	0.004
> 1 metastatic site	1.34	(1.00, 1.80)	0.048
Synchronous metastasis	0.81	(0.62, 1.07)	0.141
Secondary metastasis surgery	0.32	(0.19, 0.52)	< 0.001
ALP > UNL	1.83	(1.37, 2.44)	< 0.001
<i>BRAFV600E</i> mutation	1.61	(1.03, 2.52)	0.036
<i>KRAS</i> mutation	1.60	(1.17, 2.18)	0.003
CDX2 negative	1.74	(1.12, 2.70)	0.013
MSI-H	3.35	(1.64, 6.84)	0.001
CD3 high	0.73	(0.55, 0.97)	0.029
CD68 high	0.61	(0.46, 0.81)	0.001

*Abbreviations:* n: number of patients; e: number of events; HR: hazard ratio; CI: confidence interval; p-value: from likelihood ratio test; PS ECOG: performance status score developed by Eastern Cooperative Oncology Group; Right-sided tumour: Site of colon cancer in ascending colon and transversum; Synchronous metastases: within six months after initial diagnoses; ALP > UNL: Alkaline Phosphatase above upper normal limit; MSI-H: microsatellite instable high; CD3 high: density of tumour infiltrating CD3 lymphocytes > median value; CD68 high: density of tumour infiltrating CD68 macrophages > median value

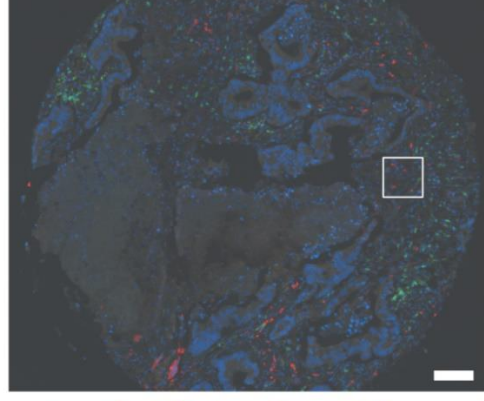
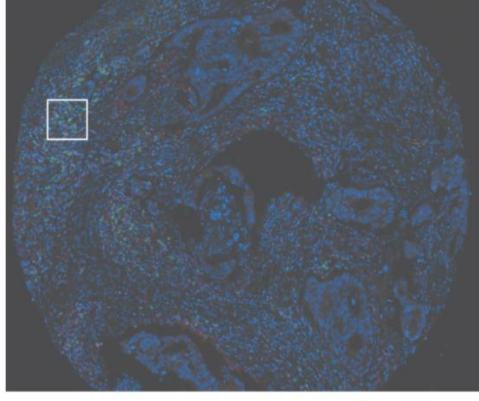
**TABLE S7** Results from Cox regression of overall survival according to MSI, BRAF and CDX2 status in subgroups with high (> median) and low density of tumour infiltrating CD3 lymphocytes and CD68 macrophages in a Scandinavian population-based cohort of metastatic colorectal cancer patients

Variable	MSI				BRAFV600E mutated				CDX2 loss			
	n (%)	HR	95 % CI	p-value	n (%)	HR	95 % CI	p-value	n (%)	HR	95 % CI	p-value
CD3 low	9 (4)	2.24	(1.13, 4.44)	0.021	41 (18)	1.60	(1.13, 2.26)	0.007	41 (18)	2.34	(1.64, 3.33)	< 0.001
CD3 high	26 (12)	2.85	(1.86, 4.36)	< 0.001	50 (22)	1.80	(1.31, 2.49)	< 0.001	42 (19)	2.10	(1.48, 2.98)	< 0.001
CD68 low	15 (7)	1.51	(1.08, 2.09)	0.015	45 (20)	1.51	(1.08, 2.09)	0.015	39 (18)	2.00	(1.40, 2.85)	< 0.001
CD68 high	20 (9)	2.52	(1.56, 4.07)	< 0.001	46 (21)	1.86	(1.33, 2.59)	< 0.001	44 (19)	2.39	(1.69, 3.38)	< 0.001

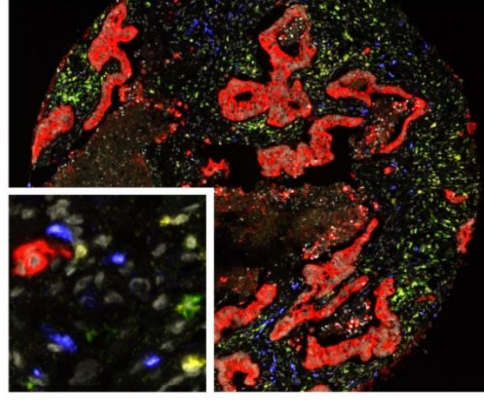
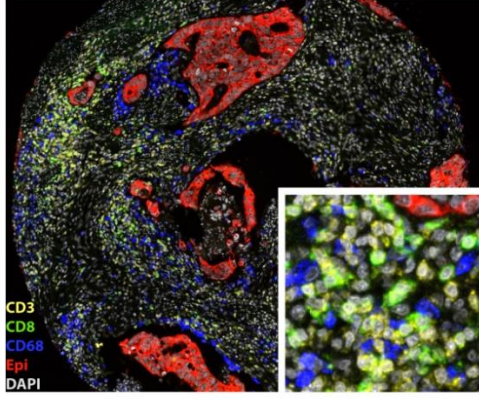
*Abbreviations:* n: number of patients with MSI, BRAF mutation or CDX2 loss; HR: hazard ratio; CI: confidence interval; p-value: from likelihood ratio test; MSI: microsatellite instable high

**FIGURE S1** Representative examples from the inForm software image analysis. Raw images (top, white boxes indicate zoomed in portions of the images) were spectrally unmixed (middle top). Tissue autofluorescence was also unmixed in this step (omitted here for visualization purposes). Based on a user-trained machine learning algorithm, the tissue was segmented into specified categories (middle bottom). Finally, individual nuclei were segmented based on the DAPI signal (bottom), and cytoplasmic and membrane segmentation were aided by signals from CD68, CD3, CD8 and the epithelial markers, as described in the methods section. Signal detected within the nuclear area was used to score cells as CD3 and/or CD8 positive, while signal within the entire cell was used to score cells as CD68 positive (described in the methods section). Only nuclear segmentation is included in the figure for visualization purposes. All images were reviewed after batch analysis and regions of necrosis, folds or poor quality were excluded (illustrated by the dark regions in the tissue and cell segmentation maps for the core on the right). Scale bar equals 100  $\mu\text{m}$  in the images of the cores, while the portions in the lower corners are 5x further zoomed.

Raw multispectral  
RGB image

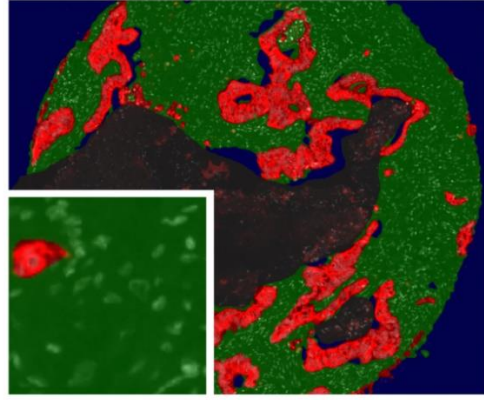
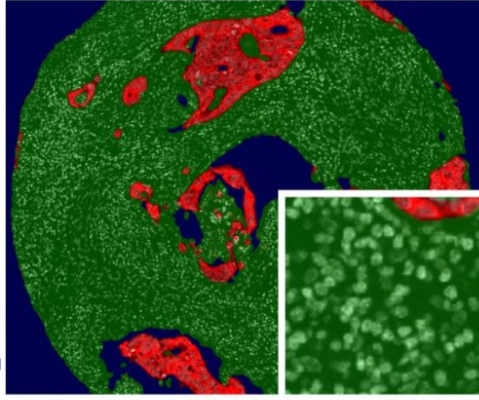


Spectrally unmixed  
image



Tissue segmentation  
map

Epithelium  
Stroma  
Background  
Excluded



Cell segmentation  
map

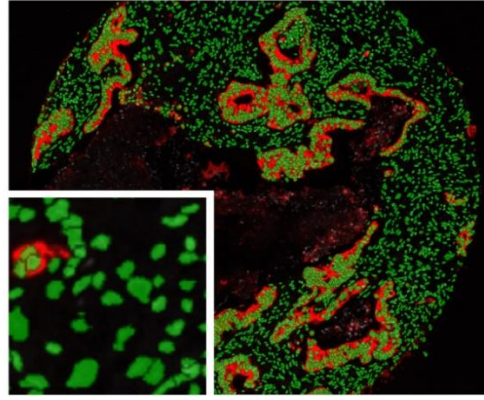
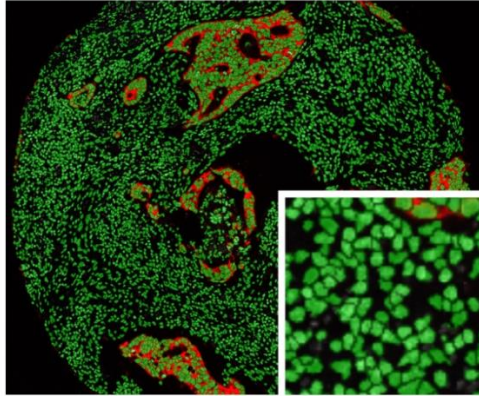


**Figure S2** Scatter plots demonstrating the correlation of immune cell density between two tumour cores taken from each patient in the generation of tissue microarray (TMA) in a Scandinavian population-based cohort of metastatic colorectal cancer patients (n=436). A) density of whole tissue CD3 lymphocytes B) density of whole tissue CD8 lymphocytes C) density of stroma CD68 macrophages. Abbreviations: p-value: determined by Spearman's rank correlation; rho; Spearman's rank correlation coefficient.

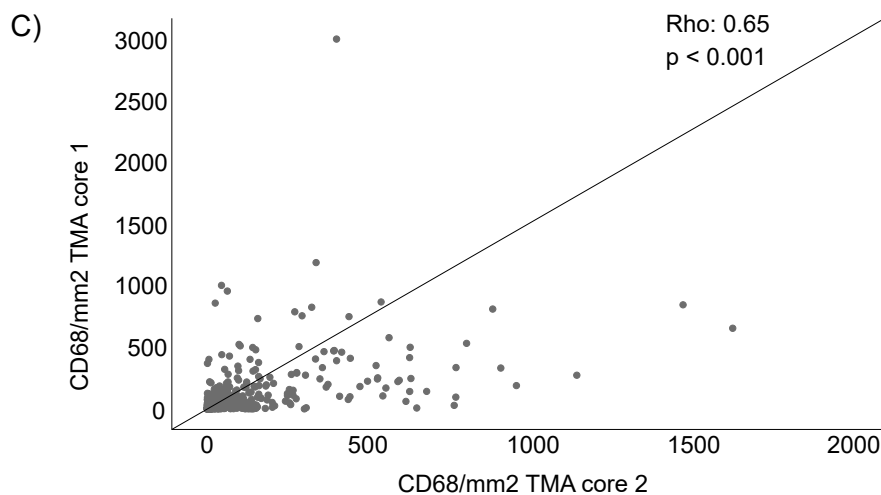
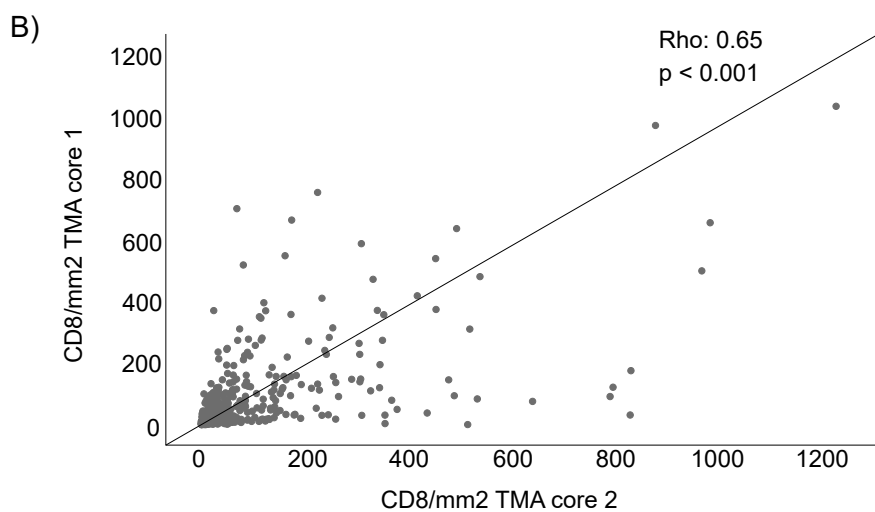
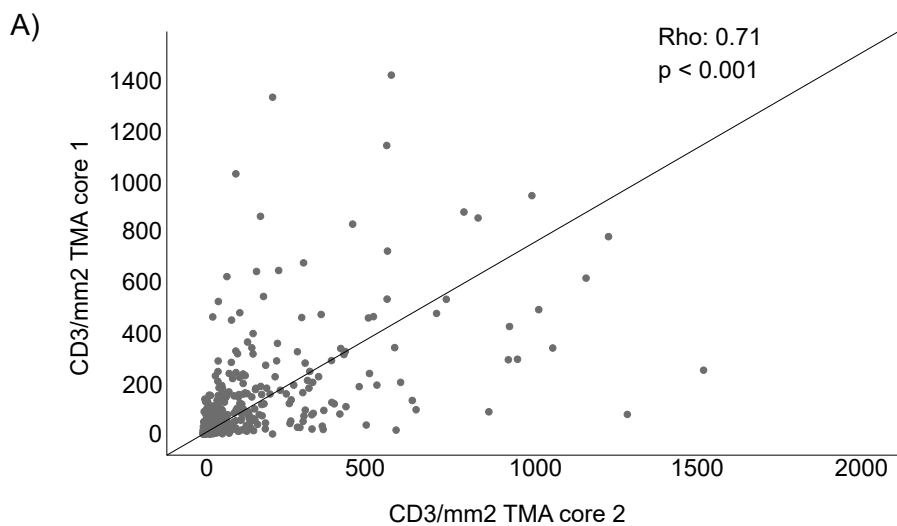


**FIGURE S3** Overall survival (OS) according to high (>median) vs low tumour infiltration of CD3 lymphocytes and CD68 macrophages and tumour molecular alterations in a Scandinavian population-based cohort of metastatic colorectal cancer treated with 1st-line chemotherapy. Kaplan-Meier curves were constructed, statistical significance test with the log-rank test for p-value and univariate cox regression for hazard ratio (HR) and 95% confidence interval (CI). A) OS of tumour infiltrating CD3 lymphocytes in subgroups of MSI and MSS cases B) OS according to tumour infiltrating CD3 lymphocytes in subgroups of *BRAF* mutated and wildtype cases C) OS according to tumour infiltrating CD3 lymphocytes in subgroups of CDX2 positive and negative cases D) OS of tumour infiltrating CD68 macrophages in subgroups of MSI and MSS cases E) OS according to tumour infiltrating CD68 macrophages in subgroups of *BRAF* mutated and wildtype cases F) OS according to tumour infiltrating CD68 macrophages in subgroups of CDX2 positive and negative cases

